Food Chemistry: X 32 (2025) 103376

Contents lists available at ScienceDirect

Food Chemistry: X

journal homepage: www.sciencedirect.com/journal/food-chemistry-x

Phytochemical profiling of *Lepidium apetalum* using GC/LC-MS metabolomics coupled with chemometric and bioactivity analyses

Fengke Lin [a], Qun Zhou [a], Guochen Lin [b], Zihao Liu [a], Rui Zhao [a], Binsheng Luo [c,*]

[a] School of Chemistry and Chemical Engineering, Tianjin University of Technology, Tianjin 300384, China
[b] Department of Physical and Chemical Laboratory Testing, Feicheng Center for Disease Control and Prevention, Feicheng 271600, China
[c] Lushan Botanical Garden, Jiangxi Province and Chinese Academy of Sciences, Lushan 332900, China

ARTICLE INFO

Keywords:
Lepidium
Chemical compositions
Bioactivities
Metabolomics
Chemometrics
Nutraceutical potential

ABSTRACT

Lepidium apetalum is valued for its food and medicinal uses; however, research on its chemistry and bioactivities remains limited. This study investigated volatile oils (VOs) and non-volatile extracts (NVEs) from different plant parts. GC–MS identified 111 volatiles dominated by nitrogen- (1.99–70.38 % across plant parts), sulfur- (5.65–62.07 %), and terpenoid-type compounds (0.28–61.06 %). UPLC-QE-Orbitrap-HRMS characterized 573 metabolites, including fatty acids, amino acids, and phenylpropanoids. PCA and PLS-DA revealed significant metabolic differences, identifying 26 differential compounds from GC–MS and 88 from LC-MS. Bioactivity variations were notable: root and husk VOs showed the strongest NO inhibition (IC_{50} 1.34–2.24 μg/mL), leaf NVE was most active against HL-60 cells (IC_{50} 82.10 μg/mL), and seed and husk extracts exhibited the highest antioxidant activity (IC_{50} 143.69–874.43 μg/mL). Correlation analysis identified key metabolites, including benzyl isothiocyanate and erucin, as strongly linked to bioactivities. These findings expand phytochemical knowledge of *L. apetalum* and highlight its potential for food and nutraceutical applications.

1. Introduction

Lepidium L. (Brassicaceae), the second largest genus of the family, comprises about 250 species distributed worldwide except Antarctica (Al-Shehbaz, 2012). Several species, such as *L. sativum*, are valued for their nutritional and nutraceutical properties, showing promising potential for applications in the dairy and food industries (Lahiri & Rani, 2020). Phytochemical studies on this genus resulted in the identification of diverse secondary metabolites including flavonoids, alkaloids, cardiac glycosides, and volatiles (Al-Snafi, 2019). Biological assays further demonstrated that the crude extracts and compounds from *Lepidium* plants exhibit various activities, including antioxidant, anti-inflammatory, and anticancer effects (Al-Snafi, 2019; Getahun et al., 2020).

Lepidium apetalum Willd., one of the 16 recorded *Lepidium* species in China, is commonly known as "*Du Xing Cai*" in Chinese and mainly distributed in northern, northeastern, and southwestern regions (Zhang et al., 2020). This species has several food uses: the leaves and stems are eaten as a wild vegetable or used in soups and cold dishes; young seedlings can be added to salads; and the appetite-stimulating seeds are used as a spice (Commission of Chinese Ethnomedicines, 2005; Zhang, 2000). Additionally, the whole plant and seeds can be used to treat many disorders such as rheumatic arthritis, hypertension edema, and conjunctivitis (Commission of Chinese Ethnomedicines, 2005), highlighting its potential as a functional food.

Despite its recognized food and medicinal value, research on the chemistry and bioactivity of *L. apetalum* remains scarce. Research has predominantly focused on the phytochemistry and bioactivity of seed non-volatile extracts (NVEs) (Shi et al., 2015; Yuan et al., 2017), with far less attention given to other plant parts such as leaves, stems, and roots. Although volatile oils (VOs) containing sulfur and nitrogen compounds have been identified in *L. apetalum* seeds (Zhao et al., 2005), their bioactivities remain uninvestigated. Since bioactive constituents can vary substantially between different plant parts, understanding these metabolic differences is essential for the optimal utilization of food and medicinal plants (Lin et al., 2023; Ren et al., 2025). To our knowledge, a comprehensive study integrating chemical profiling and bioactivity evaluation across multiple parts of *Lepidium* species has not been reported.

Gas chromatography mass spectrometry (GC–MS) is widely used for profiling plant VOs (Gargi et al., 2025), while Ultra-performance liquid chromatography coupled with Q-Exactive Orbitrap high-resolution mass

* Corresponding author.
E-mail address: luobins@lsbg.cn (B. Luo).

https://doi.org/10.1016/j.fochx.2025.103376
Received 24 August 2025; Received in revised form 3 December 2025; Accepted 3 December 2025
Available online 4 December 2025

spectrometry (UPLC-QE-Orbitrap-HRMS) has proven highly effective for characterizing metabolites in NVEs with excellent resolution and accuracy (Li et al., 2023). Untargeted metabolomics approaches employing GC–MS or LC-MS, combined with chemometric analyses such as principal component analysis (PCA) and partial least squares discriminant analysis (PLS-DA), allow comprehensive metabolite profiling and identification of discriminative molecules (Lin & Long, 2023; Pang et al., 2023). For example, GC–MS-based metabolomics coupled with PLS-DA revealed seasonal variations in VOs of *Garcinia xanthochymus* and *G. yunnanensis*, identifying 118 constituents and 34 differential compounds (Lin & Long, 2023). Similarly, UPLC-QE-Orbitrap-HRMS metabolomics identified 382 metabolites in *Panax quinquefolius* and highlighted 20 potential markers distinguishing geographical origins (Pang et al., 2023). Although GC–MS (Xu et al., 2011) and LC-MS (Gallegos-Saucedo et al., 2024) have been applied to *L. apetalum*, neither technique combined with chemometric analysis has been used for this species. Furthermore, the UPLC-QE-Orbitrap-HRMS approach has not yet been applied to the chemical profiling of any *Lepidium* species.

In this study, we performed a comprehensive chemical characterization of *L. apetalum* using GC–MS and UPLC-QE-Orbitrap-HRMS-based untargeted metabolomics, coupled with chemometric analyses, to profile both VOs and NVEs from different plant parts. Comparative bioactivity assays, including cytotoxicity, anti-inflammatory, and antioxidant evaluations, were performed, and correlations between metabolites and bioactivities were assessed to elucidate the observed effects and identify potential functional constituents. This study expands the phytochemical and pharmacological understanding of *L. apetalum* and provides a foundation for its development as a resource for food and nutraceutical applications.

2. Materials and methods

2.1. Chemicals and reagents

Analytical-grade methanol for extraction was purchased from Concord Technology (Tianjin, China). For GC/LC-MS analyses, HPLC-grade *n*-hexane and LC-MS-grade methanol, acetonitrile, and isopropanol were obtained from CNW Technologies GmbH (Dusseldorf, Germany). LC-MS-grade acetic acid and an *n*-alkane (C_7-C_{40}) standard mixture were supplied by Sigma-Aldrich (Saint Louis, USA), and ultrapure water was provided by Watsons (Hong Kong, China). For biological evaluation, dimethyl sulfoxide (DMSO), Dulbecco's modified eagle medium (DMEM), and Roswell Park Memorial Institute (RPMI)-1640 medium were purchased from Boehringer Ingelheim (Ingelheim, Germany). Doxorubicin (DOX) was obtained from Meilunbio (Dalian, China). 3-(4,5-Dimethylthiazol-2-yl)-5-(3-carboxymethoxyphenyl)-2-(4-sulfopheny)-2*H*-tetrazolium (MTS) was procured from Promega (Madison, USA). Griess reagent, lipopolysaccharide (LPS), and monomethylated L-arginine (L-NMMA) were purchased from Sigma-Aldrich (Saint Louis, USA). 2,2-Diphenyl-1-picrylhydrazyl (DPPH), 2,2′-azinobis-(3-ethylbenzothiazoline-6-sulfonate) (ABTS), and analytical-grade ethanol were obtained from Macklin (Shanghai, China). L-ascorbic acid (LAA) and potassium persulfate ($K_2S_2O_8$) were sourced from Aladdin (Shanghai, China).

2.2. Plant materials

Whole plants of *L. apetalum* were collected in May 2024 from Xiqing District, Tianjin, China, with GPS coordinates as follows: 1 m (above sea level), 39°3′59.89″ N, 117°8′30.28″ E. Species identification was initially performed by the first author and subsequently verified by Xingxing Chen, Lushan Botanical Garden, Chinese Academy of Sciences, Jiangxi Province, China. After collection, the plants were manually separated into five parts: roots (LA-R), stems (LA-St), leaves (LA-L), seeds (LA-S), and husks (LA-H). Each plant part was naturally air-dried under light-protected conditions, finely ground, and passed through a 40-mesh sieve. The resulting homogeneous powders were labeled with their respective part codes and stored in the dark at −20 °C until extraction.

2.3. Preparation of VOs and NVEs from L. apetalum

VOs from various parts of *L. apetalum* were obtained by hydrodistillation using a Clevenger apparatus. Approximately 100 g of the sample was placed into a 2000 mL round-bottom flask containing 1000 mL of deionized water and several glass beads to prevent overboiling. The mixture was sonicated for 30 min, then gently heated using an electric heating mantle (Beijing Ever-Bright Medical Treatment Instrument Co., Ltd., Beijing, China) and maintained at a gentle boil for about 6 h, until no further increase in oil volume was observed in the receiver. The volumes of VOs were measured and their contents were calculated as the ratio of oil volume (mL) to the dry weight of the sample (g) (*v/w*, %).

NVEs from different plant parts were prepared using a solvent extraction method (Ren et al., 2025). Each plant part sample (3.0 g) was extracted with 100 mL of methanol under sonication for 20 min and then filtered through filter paper to collect the supernatant. The extraction was repeated three times, and all supernatants from the same part were combined and concentrated under reduced pressure using a rotary evaporator (RE-2000, Tianjin Kenuo Instrument Equipment Co., Ltd., Tianjin, China). The concentrated extracts were subsequently freeze-dried using an LGJ-10C lyophilizer (Sihuan Forui Technology Development Co., Ltd., Beijing, China) for 48 h to completely remove the solvent. The dried extracts were stored at −20 °C until further analysis.

2.4. GC–MS analysis

The chemical composition of VOs from *L. apetalum* was analyzed using a GC-2030 gas chromatograph coupled with a QP2020 NX mass spectrometer (Shimadzu, Kyoto, Japan). Prior to analysis, each VO sample was dissolved in *n*-hexane (1 mg/mL) and ultrasonically treated in an ice-water bath for homogenization. A pooled quality control (QC) sample was prepared by combining 30 μL aliquots from each VO sample. Chromatographic separation was performed on a DB-5 MS capillary column (30 m × 250 μm, 0.25 μm film thickness; J&W Scientific, Folsom, USA) using helium as the carrier gas at a constant flow rate of 1 mL/min, with an injection of 5 μL and a front inlet purge flow of 3 mL/min. The oven temperature program was initiated at 50 °C (held for 1 min), then increased at a rate of 8 °C/min to 310 °C (held for 11.5 min). The injection port, transfer line, and ion source temperatures were set at 280 °C, 280 °C, and 230 °C, respectively. Mass spectrometry was performed in electron impact (EI) mode at 70 eV with a mass scan range of *m/z* 50–500 and an acquisition rate of 12.5 spectra per second. Raw data were processed using Leco Chroma TOF software (V4.3×) for baseline correction, peak detection, alignment, deconvolution, and integration. Linear retention indices (LRIs) were calculated using a standard mixture of *n*-alkanes (C_7-C_{40}) as references. Compound identification was accomplished by matching mass spectra with the NIST23 database and comparing LRIs with literature values (Adams, 2017) and reference data from the NIST Chemistry WebBook (https://webbook.nist.gov/chemistry/). The relative abundance (%) of each VO was calculated based on its peak area relative to the total ion chromatogram of the corresponding plant part.

2.5. UPLC-QE-Orbitrap-HRMS analysis

Each NVE sample was dissolved in methanol (1 mg/mL), sonicated for 10 min, and centrifuged at 12,000 rpm for 15 min to obtain clear supernatants for LC-MS analysis. A QC sample was prepared by mixing equal volumes (30 μL) from each sample. Metabolite profiling of the NVE samples was performed using a Vanquish UPLC system (Thermo Fisher Scientific, Waltham, USA) coupled with a QE Orbitrap Exploris

120 mass spectrometer (Thermo Fisher Scientific). Chromatographic separation was achieved on a Phenomenex Kinetex C_{18} column (2.1 mm × 100 mm, 2.6 μm) with mobile phase A (water containing 0.01 % acetic acid) and mobile phase B (isopropanol: acetonitrile, 1:1, *v/v*). The autosampler temperature was maintained at 4 °C, and 2 μL of each sample was injected. The gradient elution program was as follows: 0–1 min (1 % B), 1–8 min (1–99 % B), 8–11 min (99 % B), 11–11.1 min (99–1 % B), and 11.1–12 min (1 % B). High-resolution mass spectrometry parameters were set as follows: sheath gas flow, 50 arbitrary units; auxiliary gas flow, 15 arbitrary units; sweep gas flow, 1 arbitrary unit; capillary temperature, 320 °C; vaporizer temperature, 350 °C; full MS resolution, 60,000; MS/MS resolution, 15,000; stepped normalized collision energies, 20, 30, and 40 eV; spray voltage, +3.8 kV in positive mode and − 3.4 kV in negative mode. Data processing involved conversion of raw files to mzXML format using ProteoWizard software (version 3.0.24054), followed by peak detection, alignment, and integration using an in-house R script based on XCMS. Metabolites were identified by matching their retention times and acquired MS/MS spectra with entries in the in-house BiotreeDB (version 3.0), which contains reference spectra obtained from authentic standards analyzed under identical LC-MS conditions.

2.6. Anti-inflammatory assays

The anti-inflammatory activity was evaluated using LPS-stimulated RAW 264.7 murine macrophages. RAW 264.7 cells were seeded into 96-well plates at a density of 8×10^4 cells per well and cultured in DMEM for 24 h. After incubation, test extracts (100 μg/mL) were added, followed by LPS at a final concentration of 1 μg/mL to induce stimulation. L-NMMA at a final concentration of 12.4 μg/mL was used as a positive control. After an additional 24 h of incubation, 50 μL of the culture supernatant was mixed with 100 μL of Griess reagent to quantify nitric oxide (NO) production by measuring absorbance at 570 nm. Inhibition of NO production was calculated using the formula: inhibition (%) = $[1 - (OD_{sample} - OD_{blank})/(OD_{LPS} - OD_{blank})] \times 100$, where OD_{sample} is the absorbance of the group treated with both LPS and extracts, OD_{blank} represents the absorbance of untreated group without LPS and extracts, and OD_{LPS} denotes the absorbance of the LPS-stimulated group. To assess cell viability and exclude compound-related cytotoxic effects, 20 μL of MTS reagent was added to the remaining cells. Cytotoxic extracts that reduced RAW 264.7 cell viability to below 90 %, including VOs of LA-R, LA-S and LA-H, were serially diluted two-fold until non-toxic concentrations were obtained for NO inhibition assessment. For *L. apetalum* VOs or NVEs exhibiting >50 % NO inhibition without cytotoxicity, their half-maximal inhibitory concentrations (IC_{50}) were subsequently determined through concentration-response experiments using five different doses: 0.39, 0.78, 1.56, 3.13, and 6.25 μg/mL for LA-R and LA-H VOs; 3.13, 6.25, 12.5, 25, and 50 μg/mL for LA-S VO; and 6.25, 12.5, 25, 50, and 100 μg/mL for LA-St and LA-L VOs as well as LA-L NVE.

2.7. Cytotoxicity evaluation

The cytotoxic potential of VOs and NVEs from *L. apetalum* was evaluated against five cancer cell lines, including lung cancer A549, human myeloid leukemia HL-60, human hepatoma HepG2, breast cancer MDA-MB-231, and human colon cancer SW480, using the MTS assay. Cells were cultured in RPMI-1640 or DMEM at 37 °C in a humidified atmosphere containing 5 % CO_2. For the assay, cells were seeded in 96-well plates at the following densities: 3000 cells/well for A549, 5000 cells/well for HepG2, MDA-MB-231, and SW480, and 15,000 cells/well for HL-60. After incubation for 12–24 h, the culture medium was removed and the test extracts were added at a final concentration of 100 μg/mL in triplicate, with DOX (1.0 μg/mL) serving as positive controls. Following 48 h of incubation, the medium was removed, and 20 μL of MTS reagent, along with 100 μL of fresh medium, was added to each well. After an additional 2–4 h of incubation (2 h for A549 and HepG2; 3 h for MDA-MB-231 and SW480; and 4 h for HL-60), the optical density (OD) was measured at 492 nm. The cytotoxicity was evaluated using the formula: cell inhibition (%) = $[1 - (OD_{sample} - OD_{blank})/(OD_{control} - OD_{blank})] \times 100$, where OD_{sample} is the absorbance of extract-treated cells, $OD_{control}$ denotes the absorbance of DMSO-treated cells, and OD_{blank} represents the absorbance of medium containing the MTS reagent without cells. For LA-L NVE exhibiting >50 % inhibition, IC_{50} values were further measured through concentration-response experiments using five different doses: 6.25, 12.5, 25, 50, and 100 μg/mL.

2.8. Antioxidant assessments

The antioxidant activities of *L. apetalum* extracts were assessed using the DPPH radical scavenging and ABTS radical cation decolorization assays. For the DPPH assay, a freshly prepared 0.1 mM DPPH solution in methanol was used. Each extract (20 μL) was mixed with 180 μL of DPPH solution in 96-well plates, resulting in final concentrations of 1600 μg/mL for VOs and 800 μg/mL for NVEs. For the ABTS assay, ABTS radical cation was generated by incubating 7 mM ABTS with 2.45 mM $K_2S_2O_8$ in the dark for 12–16 h, followed by dilution with ethanol to an absorbance of 0.70 ± 0.02 at 734 nm. Similarly, 20 μL of each extract solution was added to 180 μL of the ABTS radical solution in a 96-well plate, yielding final concentrations of 1600 μg/mL for VOs and 800 μg/mL for NVEs. LAA (10 μg/mL) was used as a positive control and DMSO (20 μL) served as the negative control. All reactions were performed in triplicate and incubated at 37 °C in the dark for 30 min. Absorbance was measured at 517 nm (DPPH) and 734 nm (ABTS) to determine radical scavenging activity, calculated using the formula: inhibition (%) = $(1 - OD_{sample}/OD_{control}) \times 100$, where OD_{sample} represents the absorbance of the extract-treated group and $OD_{control}$ denotes the absorbance of the negative control group. Extracts showing >50 % scavenging activity in the assay were further analyzed to determine their IC_{50} values through concentration-response experiments using five different doses: 100, 200, 400, 800, and 1600 μg/mL for LA-S and LA-H VOs; and 50, 100, 200, 400, and 800 μg/mL for the NVE samples.

2.9. Statistical analysis

PCA and PLS-DA analyses were conducted using SIMCA-P 14.1 software (Umetrics, Umea, Sweden). The variable importance in projection (VIP) values for detected features were derived from the PLS-DA model and *p*-values were obtained via one-way ANOVA using IBM SPSS Statistics 27.0 (IBM, Chicago, USA). Features with *p*-values lower than 0.05 and VIP values greater than 1.3 were considered as significantly differential metabolites (Wu et al., 2023). For the bioactivity assays, data were expressed as mean ± standard deviation (SD) and IC_{50} values were calculated using GraphPad Prism (version 10.05). The statistical significance of experimental results was analyzed by one-way ANOVA with Duncan's multiple comparison test in IBM SPSS Statistics, where $p < 0.05$ was considered statistically significant between groups.

3. Results and discussion

3.1. Chemical compositions of VOs using GC–MS analysis

Hydrodistillation of different parts of *L. apetalum* yielded VOs ranging 0.09 % to 0.35 %, with the highest yield obtained from LA-R (0.35 %), followed by LA-S (0.17 %), LA-L (0.14 %), and LA-H (0.12 %) (**Fig. S1**). A previous study reported a VO yield of 0.15 % from *L. apetalum* seeds using the hydrodistillation method (Gong et al., 2015), which is comparable to our result (0.17 %). To our knowledge, this is the first report on the VO yields of non-seed parts of *L. apetalum*. GC–MS analysis identified 111 volatile constituents, classified into 11 chemical groups including terpenoids, sulfur- or nitrogen-containing compounds,

and esters (Table 1). Among them, nitrogen-containing compounds were the most abundant, with relative abundances ranging from 1.99 % to 70.38 % across different plant parts, followed by sulfur-containing compounds (5.65–62.07 %), terpenoids (0.28–61.06 %) and fatty acids (0.02–42.58 %) (**Fig. S2**). Notably, nitrogen- and sulfur-containing compounds predominated in LA-R (94.04 %), LA-S (90.40 %), and LA-H (79.67 %), whereas terpenoids and fatty acids were more enriched in LA-L (63.71 %) and stems (LA-St, 60.94 %) (**Fig. S2**). The prevalence of nitrogen- and sulfur-containing volatiles has also been reported in other *Lepidium* species, such as *L. meyenii* and *L. sativum* (Getahun et al., 2020; Tellez et al., 2002), indicating that *Lepidium* VOs are rich sources of these specialized metabolites.

At the individual compound level, the dominant VOs in the LA-R were phenylacetonitrile (69.62 %), 5-(methylsulfanyl)pentanenitrile (11.65 %), erucin (7.73 %), benzyl isothiocyanate (2.47 %), and 6-(methylthio)hexanenitrile (1.15 %) (Table 1). In LA-S, phenylacetonitrile (40.85 %) was also the major constituent, followed by dibenzyl disulfide (16.34 %), 5-(methylsulfanyl)pentanenitrile (10.24 %), benzenemethanethiol (8.27 %), and benzyl methyl disulfide (6.09 %). The LA-H oil shared several dominant components with LA-S, including phenylacetonitrile (14.59 %), dibenzyl disulfide (4.89 %), and 5-(methylsulfanyl)pentanenitrile (3.59 %), with erucin (44.19 %) and benzyl isothiocyanate (4.94 %) also abundant (Table 1). In contrast, LA-St was dominated by *n*-hexadecanoic acid (42.47 %), phytol (7.43 %), dibenzyl disulfide (4.88 %), methyl hexadecanoate (4.01 %), and 6,10,14-trimethylpentadecan-2-one (3.94 %). LA-L contained high levels of phytol (18.50 %), 6,10,14-trimethylpentadecan-2-one (11.05 %), trans-β-ionone (9.25 %), 10-(acetylmethyl)-(+)-3-carene (6.89 %), and dehydrodihydroionone (5.47 %). Previous studies on *L. apetalum* seeds reported phenylacetonitrile (84.87 %), 5-(methylsulfanyl)pentanenitrile (6.25 %), and dibenzyl disulfide (3.17 %) as major volatiles (Zhao et al., 2005), consistent with our findings. However, Gong et al. (2015) identified 4-(chloromethyl)benzonitrile (88.9 %), 2-pyridinecarbonitrile (2.72 %), and methyl 6,9-octadecadienoate (1.59 %) as dominant seed VOs, also using the extraction method of hydrodistillation. Such discrepancies in seed VO profiles of *L. apetalum* may result from differences in genotype, geographic origin, or harvest period. Several dominant compounds, including phenylacetonitrile, benzyl isothiocyanate, and *n*-hexadecanoic acid, have also been reported in *L. sativum* VOs (Afsharypuor & Hadi, 2006); however, phenylacetonitrile, the major component in LA-R oil in this study (69.62 %), was absent in *L. sativum* root VO (Afsharypuor & Hadi, 2006), highlighting similarities and differences within the *Lepidium* genus. This study provides the first comprehensive characterization of VOs from the roots, stems, leaves, and hulls of *L. apetalum*, thereby expanding the chemical knowledge of this species beyond its seeds. However, future research is needed to investigate how other factors, such as seasonal and geographical variations, affect the metabolite profiles of *L. apetalum*, to guide its optimal utilization.

3.2. Chemical compositions of NVEs by UPLC-QE-orbitrap-HRMS

Nontargeted metabolomic analysis of NVEs of *L. apetalum* using UPLC-QE-Orbitrap-HRMS resulted in the annotation of 573 metabolites, with 272 detected in positive mode and 377 in negative mode (**Table S1**). These metabolites were grouped into 11 major chemical classes, predominantly fatty acids and derivatives (129 compounds), amino acids and peptides (78), phenylpropanoids (65), glycerophospholipids (54), alkaloids (51), and flavonoids (47) (**Fig. S3**). Many identified metabolites have been documented to exert diverse biological activities. For instance, the phenylpropanoid rosmarinic acid (Alagawany et al., 2017), the phenolic acid vanillic acid (Sharma et al., 2020), and the flavonoid rutin (Gullón et al., 2017) have been widely recognized for their therapeutic properties, including anti-inflammatory, antioxidant, neuroprotective, and anti-obesity effects. These findings provide a comprehensive chemical profile of *L. apetalum* NVEs, highlighting their potential as a natural source of both nutritional and bioactive compounds for food applications.

3.3. Metabolite variations among VO and NVE samples

To provide an overview of metabolite variations across different plant parts, all the detected molecules of VOs and NVEs were analyzed using PCA and PLS-DA. In the PCA score plots (Figs. 1A-1C), the cumulative R^2X and Q^2 values both exceeded 0.5 (**Table S2**), indicating good explanatory and predictive power and confirming the model's validity. In the PLS-DA plots, the cumulative R^2X, R^2Y, and Q^2 values all exceeded 0.9 (**Table S2**), indicating excellent model fit and predictive ability. Additionally, the permutation tests for all PLS-DA models yielded negative Q^2 *y*-intercepts (**Fig. S4**), further confirming the robustness and absence of overfitting of the constructed model. QC samples clustered near the center in all plots, suggesting stable and reproducible analytical performance (Fig. 1).

As shown in Fig. 1, both PCA and PLS-DA plots separated VOs (detected by GC–MS) and NVEs (analyzed by UPLC-QE-Orbitrap-HRMS in positive and negative modes) from other samples, indicating significant metabolic differences among the plant parts of *L. apetalum*. These results demonstrate that GC–MS- or LC-MS-based metabolomics combined with chemometric analysis is effective for discriminating different plant parts of *L. apetalum*. Similar findings have been reported in other species, such as *Fissistigma polyanthum* (Ren et al., 2025) and *Garcinia subfalcata* (Lin et al., 2025), where chemometric approaches also revealed marked chemical variations among plant organs. Although PLS-DA has previously been applied to differentiate extracts from dry roots and commercial products of *L. meyenii* (Carvalho et al., 2021), this is, to our knowledge, the first study to uncover chemical differences among plant parts of *Lepidium* species using chemometric analysis.

Although metabolites with VIP values greater than 1 are generally considered important for discriminating differences among groups in multivariate analyses, higher VIP thresholds, such as 1.3 and 1.5, are often applied to focus on compounds with stronger discriminatory power while maintaining a manageable number of metabolites (Lin & Long, 2023; Ren et al., 2025; Wu et al., 2023). In the current study, variables with VIP values >1.3 from the PLS-DA model and $p < 0.05$ from ANOVA were characterized as key discriminative metabolites (Wu et al., 2023). A total of 114 discriminative compounds were identified, including 26 from VO samples (Table 2), 53 from NVE samples in LC-MS positive mode, and 35 from NVE samples in LC-MS negative mode (Table 3). In VOs, the top discriminating metabolite was *n*-hexadecanoic acid with a VIP value of 9.43, followed by erucin (9.13) and phenylacetonitrile (8.76) (Table 2). For NVEs in positive mode, the most discriminating metabolites were LPC(18:4) (1.78), 4-(4′-methyl-[2,2′-bipyridin]-4-yl)butanoic acid (1.77), and 4-*O*-feruloyl-D-quinic acid (1.73). In negative mode, the top markers were stachyose (1.83), tryptophan (1.81), and ursolic acid (1.68) (Table 3). To our knowledge, this study provides the first report of significantly discriminating metabolites among different parts of *L. apetalum*. Previous studies showed that metabolomics combined with chemometric methods such as PLS-DA can effectively identify key differential metabolites, enabling authentication of plant-derived products (Abraham & Kellogg, 2021). The discriminative compounds identified in the current study provide insights into the chemical differences among plant parts of *L. apetalum* and may serve as valuable markers for verifying medicinal products derived from specific plant parts. Among the characterized metabolites, several, such as *n*-hexadecanoic acid (Ravi & Krishnan, 2017) and linarin (Mottaghipisheh et al., 2021), identified through GC–MS or LC-MS analyses, possess diverse bioactivities, including cytotoxic, antioxidant, and antibacterial effects. Variations in the abundance of these bioactive compounds may affect the therapeutic potential of different *L. apetalum* organs.

Table 1
Chemical compositions (%) of VOs from different plant parts of *L. apetalum*.

No.	Compound	LRI[a]	LRI[b]	Class[c]	VO sample[d]				
					LA-R	LA-St	LA-L	LA-S	LA-H
1	2,6,6-Trimethylcyclohexanone	1036	1036	A	tr	0.01	0.03	tr	0.01
2	3,6,6-Trimethyl-cyclohex-2-enol	1061		A	nd	0.01	0.06	nd	0.01
3	Linalool	1102	1103	A	nd	tr	0.05	tr	0.01
4	Menthol	1184		A	tr	0.02	0.03	0.01	0.01
5	Safranal	1204	1202	A	0.01	0.05	0.36	0.02	0.11
6	*β*-Cyclocitral	1225	1224	A	tr	0.05	0.24	0.01	0.03
7	2,6,6-Trimethyl-1-cyclohexene-1-acetaldehyde	1262		A	nd	0.02	0.09	nd	0.01
8	*α*-Longipinene	1334	1334	A	0.02	0.10	1.72	0.03	0.22
9	10-(Acetylmethyl)-(+)-3-carene	1391		A	0.08	0.40	6.89	0.13	0.46
10	6,10-Dimethyl-2-undecanone	1403		A	0.01	0.04	0.34	0.01	0.03
11	Dehydrodihydroionone	1415		A	0.01	0.06	5.47	0.02	0.36
12	2,2,6*β*,7-Tetramethylbicyclo[4.3.0]nona-1(9),7-dien-5-ol	1420		A	nd	0.14	0.54	nd	0.03
13	Geranylacetone	1451	1460	A	tr	0.15	0.46	tr	0.05
14	*trans*-*β*-Ionone	1464	1456	A	0.01	3.60	9.25	0.06	0.51
15	Dehydro-*β*-ionone	1481		A	0.03	0.15	0.75	0.05	0.56
16	5,6-Epoxy-*β*-ionone	1487	1473	A	tr	0.22	0.86	0.05	0.17
17	Nerolidol	1564	1565	A	0.02	0.11	0.14	0.04	0.08
18	Megastigmatrienone	1585		A	nd	nd	0.03	tr	0.07
19	(3*Z*)-2-Methyl-4-(2,6,6-trimethyl-1-cyclohexen-1-yl)-3-butenal	1586		A	0.01	0.03	0.16	0.01	0.02
20	(*E*)-Atlantone	1781	1773	A	nd	nd	0.02	nd	nd
21	Neophytadiene	1836	1836	A	tr	0.16	0.16	0.01	0.29
22	6,10,14-Trimethylpentadecan-2-one	1843	1845	A	0.04	3.94	11.05	0.04	0.68
23	Farnesyl acetone	1912	1927	A	0.01	0.77	1.80	tr	0.10
24	3-Methyl-2-(3,7,11-trimethyldodecyl) furan	1916		A	tr	0.01	0.06	tr	0.01
25	Isophytol	1947	1949	A	0.01	0.75	1.71	0.03	0.13
26	Geranyllinalool	2027		A	tr	0.06	0.17	0.02	0.01
27	Phytol	2111	2111	A	tr	7.43	18.50	0.58	0.33
28	4,8,12,16-Tetramethylheptadecan-4-olide	2351		A	tr	0.09	0.10	0.01	0.02
29	Squalene	2813	2815	A	tr	0.02	0.03	tr	0.01
30	Benzenemethanethiol	1086	1080	B	0.30	0.57	0.75	8.27	1.54
31	3,5-Dimethyl-1,2,4-Trithiolane	1155	1148	B	tr	tr	0.03	0.12	0.01
32	Benzyl methyl sulfide	1174	1183	B	0.03	0.06	0.03	0.36	0.15
33	3,6-Dimethyl-2,4,5,7-tetrathiaoctane	1179		B	0.01	0.02	0.01	0.35	0.05
34	5-(Methylsulfanyl)pentanenitrile	1206		B	11.65	1.87	1.20	10.24	3.59
35	Methyl furfuryl disulfide	1218		B	tr	0.01	0.01	0.36	0.02
36	6-(Methylthio)hexanenitrile	1320	1306	B	1.15	0.09	0.05	0.30	0.20
37	3-(Methylthio)propyl isothiocyanate	1323		B	0.02	0.04	0.03	0.03	0.31
38	Benzyl isothiocyanate	1374	1361	B	2.47	0.22	0.01	0.03	4.94
39	Benzyl methyl disulfide	1395		B	0.06	0.13	0.08	6.09	0.29
40	Erucin	1440		B	7.73	2.24	0.24	0.65	44.19
41	Phenethyl isothiocyanate	1466	1454	B	0.03	0.06	0.04	0.05	0.70
42	Berteroin	1551	1535	B	0.09	0.20	0.12	0.15	0.71
43	Phenacyl phenyl sulfide	1833		B	0.02	0.05	0.03	0.30	0.05
44	3-Ethyl-2,4,5-trithiaoctane	1914		B	nd	nd	nd	0.45	nd
45	Dibenzyl disulfide	2082	2070	B	tr	4.88	2.87	16.34	4.89
46	3-Methyl-2-(3,7,11-trimethyldodecyl)thiophene	2124		B	nd	tr	0.05	tr	tr
47	Benzyl trisulfide	2354		B	0.09	0.19	0.11	1.05	0.41
48	Methyl phenylacetate	1182	1186	C	0.01	0.01	0.01	0.17	0.01
49	Methyl 10-methylundecanoate	1524		C	0.01	0.21	0.01	nd	0.16
50	Methyl tetradecanoate	1724	1725	C	0.01	0.26	0.16	tr	0.07
51	2-Ethylhexyl salicylate	1810	1807	C	0.01	0.29	0.23	tr	0.02
52	Methyl 7,10,13-hexadecatrienoate	1896		C	0.01	0.49	1.39	0.01	0.04
53	(*Z*)-Methyl hexadec-11-enoate	1903		C	nd	0.04	0.04	nd	0.01
54	Methyl (*E*)-hexadec-7-enoate	1921		C	tr	0.02	0.02	tr	tr
55	Methyl hexadecanoate	1925	1927	C	0.08	4.01	1.96	0.55	0.82
56	Methyl linoleate	2093	2096	C	tr	0.13	0.06	0.02	0.04
57	Methyl linolenate	2099	2099	C	0.01	2.20	2.32	0.65	0.78
58	Methyl 13-octadecenoate	2104		C	tr	0.02	tr	0.03	0.01
59	(*E*)-16-Octadecenoic acid methyl ester	2105		C	tr	0.03	0.01	tr	0.02
60	Methyl isostearate	2126		C	tr	0.02	0.01	0.02	0.03
61	Ethyl linolenate	2167		C	0.03	0.06	0.14	0.14	0.34
62	5-Isopropyl-2-methylphenyl 3,5,5-trimethylhexanoate	2482		C	nd	nd	nd	nd	0.08
63	Azeleonitrile	1047		D	tr	0.11	0.04	0.38	0.06
64	1,2-Dimethyl-5-vinylpyrrole	1115		D	tr	tr	tr	0.05	tr
65	4-Ethylbenzenamine	1128		D	0.01	0.02	0.01	0.03	0.02
66	Phenylacetonitrile	1149	1148	D	69.62	1.09	1.69	40.85	14.59
67	2-Methoxy-3-(1-methylpropyl)pyrazine	1170	1172	D	0.01	tr	tr	tr	tr
68	1-Furfurylpyrrole	1185	1182	D	0.09	0.19	0.11	1.09	0.43
69	2,4-Dimethyl-3-acetylpyrrole	1233		D	0.01	0.01	0.01	0.02	0.01
70	1-Benzylpyrrole	1360		D	0.11	nd	nd	0.93	1.49
71	3-Nitrotoluene	1654		D	nd	nd	nd	1.15	0.50
72	Hexadecanenitrile	1902		D	tr	0.09	0.17	0.01	0.01
73	*N*-(2-furoyloxy)succinimide	1969		D	0.52	0.47	0.28	0.74	0.48

(*continued on next page*)

Table 1 (*continued*)

No.	Compound	LRI[a]	LRI[b]	Class[c]	VO sample[d]				
					LA-R	LA-St	LA-L	LA-S	LA-H
74	Benzeneacetaldehyde	1064	1053	E	0.01	0.01	0.01	0.01	0.04
75	3-Hydroxy-4-methylbenzaldehyde	1077		E	0.01	0.02	0.01	0.03	0.02
76	Nonanal	1108	1108	E	0.01	0.01	0.12	0.01	tr
77	2-Undecenal	1372	1373	E	0.01	0.03	0.01	0.01	0.01
78	4-Benzyloxybenzaldehyde	1615		E	0.09	0.19	0.11	0.29	0.19
79	Pentadecanal	1717	1713	E	tr	0.04	0.05	tr	tr
80	3,5-Di-*tert*-butyl-4-hydroxybenzaldehyde	1764		E	tr	0.13	0.10	0.01	0.02
81	3-(4-(Benzyloxy)phenyl)propanal	1865		E	tr	tr	tr	0.03	tr
82	Tetradecane	1399	1400	F	0.02	0.06	0.11	0.06	0.05
83	Pentadecane	1499	1500	F	0.01	0.14	0.14	0.04	0.09
84	3-Methyl-pentadecane	1571	1570	F	tr	0.01	0.01	tr	0.01
85	Hexadecane	1599	1600	F	0.02	0.43	0.45	0.08	0.37
86	Heptadecane	1698	1700	F	nd	0.01	0.01	tr	0.01
87	3-Methylheptadecane	1771	1772	F	0.01	0.19	0.06	0.02	0.04
88	Octadecane	1800	1800	F	0.01	0.11	0.18	0.02	0.06
89	Tricosane	2300	2300	F	tr	0.18	0.43	0.02	0.06
90	Butylbenzene	1056	1056	G	0.01	0.03	0.02	0.31	0.03
91	3-Ethylstyrene	1080		G	tr	0.01	0.01	0.10	0.01
92	Pentylbenzene	1162	1158	G	0.01	0.02	0.01	0.23	0.02
93	Pentenylbenzene	1231		G	tr	tr	tr	0.03	tr
94	Hexylbenzene	1265	1261	G	nd	tr	nd	0.04	tr
95	Heptylbenzene	1368		G	tr	tr	tr	0.03	tr
96	Octylbenzene	1471	1468	G	tr	0.01	0.01	tr	tr
97	1-Nonanol	1184	1174	H	0.01	0.01	tr	0.01	0.01
98	2-Hexyl-1-decanol	1515	1504	H	0.03	0.05	0.07	0.06	0.05
99	2-Hexyl-1-octanol	1543		H	0.06	0.10	0.16	0.11	0.12
100	2-Heptadecanol	1788		H	0.03	0.07	0.10	0.07	0.07
101	Tetradecanoic acid	1775	1777	I	tr	tr	tr	tr	tr
102	*n*-Hexadecanoic acid	1977	1975	I	0.01	42.47	2.61	0.01	0.16
103	Linoelaidic acid	2145		I	0.01	0.10	0.04	0.02	0.03
104	2-Methoxy-4-vinylphenol	1325	1324	J	0.09	0.20	0.12	0.15	0.48
105	5-*s*-Butylpyrogallol	1476		J	nd	nd	0.51	nd	nd
106	2,4-Di-*tert*-butylphenol	1510	1512	J	0.05	0.41	0.39	0.10	0.18
107	6-Methyl-3,5-heptadiene-2-one	1120	1105	K	nd	nd	nd	tr	0.05
108	1-Cyclopropylethanone	1134		K	0.01	0.02	0.02	0.01	0.02
109	4,6,8-Trimethyl-1-nonene	1308		K	0.15	0.28	0.42	0.29	0.33
110	1,2,3,4-Tetrahydro-1,6,8-trimethylnaphthalene	1353		K	nd	0.01	0.05	tr	0.03
111	1,1,6-Trimethyl-1,2-dihydronaphthalene	1362		K	tr	0.17	0.52	0.09	0.36
	Total (%)				95.15	84.30	82.24	95.41	89.36

[a] Linear retention index (LRI) on a DB-5 MS column, determined experimentally.
[b] Linear retention index (LRI) on a DB-5/dB-5 MS column reported in the literature or obtained from the NIST Chemistry WebBook database.
[c] Compound classes: A: terpenoids, B: sulfur-containing compounds, C: esters, D: nitrogen-containing compounds, E: aldehydes, F: alkanes, G: aromatic hydrocarbons, H: alcohols, I: fatty acids. J: phenols. K: others.
[d] VO: Volatile oil, Tr: tr: trace compounds (< 0.01 %), nd: not detected, LA: *L. apetalum*, R: roots, St: stems, L: leaves, S: seeds, H: husks.

3.4. Anti-inflammatory

Although the whole plant and seeds of *L. apetalum* have long been used in TCM to treat inflammatory disorders such as edema and rheumatic arthritis (Commission of Chinese Ethnomedicines, 2005), the anti-inflammatory properties of *L. apetalum* remain poorly studied. In this study, we systematically assessed the anti-inflammatory activities of different plant parts by evaluating their ability to suppress NO production in LPS-stimulated RAW264.7 macrophages. The results demonstrated that both VO and NVE samples from *L. apetalum* plant parts exhibited notable anti-inflammatory effects (Fig. 2). At 100 μg/mL, all VO samples markedly suppressed NO production, with inhibition rates ranging from 95.65 % to 100 % (Fig. 2A). However, cytotoxicity assays showed that LA-R, LA-S, and LA-H VOs reduced RAW 264.7 cell viability to below 90 %, suggesting that part of the strong NO inhibition could be attributed to cytotoxic effects. To more accurately assess their anti-inflammatory potential, non-toxic concentrations of the VOs were determined as follows: 6.25 μg/mL for LA-R and LA-H VOs, and 50 μg/mL for LA-S VO. Even at these reduced concentrations, LA-R, LA-H and LA-S VOs retained strong NO inhibitory effects, with inhibition rates of 98.33 %, 98.56 % and 80.78 %, respectively. IC_{50} analysis further revealed significant differences among the samples ($p < 0.05$), ranging from 1.34 to 21.91 μg/mL (Fig. 2B). Notably, LA-H ($IC_{50} = 1.34$ μg/mL) and LA-R ($IC_{50} = 2.24$ μg/mL) VOs showed the strongest activity, both significantly more potent than the positive control L-NMMA ($IC_{50} = 8.58$ μg/mL) ($p < 0.05$), highlighting their promise as natural anti-inflammatory agents. To our knowledge, this is the first to demonstrate the anti-inflammatory activity of VOs from *Lepidium* plants. These findings highlight the potential of VOs from the *Lepidium* genus as promising candidates for future anti-inflammatory research.

In contrast, NVEs exhibited less pronounced anti-inflammatory effects than their VO counterparts. Among them, LA-H NVE showed the highest activity, with 76.10 % NO inhibition, followed by LA-L NVE (42.43 %) and LA-St NVE (21.49 %) (Fig. 2C). The IC_{50} value of LA-H NVE was determined to be 58.92 ± 3.77 μg/mL. A study reported that a hydroethanolic extract of the whole *L. apetalum* plant alleviated colitis in a dextran sodium sulfate-induced model (Kim et al., 2024); however, the present study is the first to reveal the anti-inflammatory activity of specific plant parts of this species.

3.5. Cytotoxic effects

The NVEs of several *Lepidium* species have been reported to exhibit notable cytotoxic activity (Selek et al., 2018). For instance, the methanol extract of *L. sativum* significantly inhibited human colon cancer DLD-1 cells, with an IC_{50} of 110.42 μg/mL (Selek et al., 2018). However,

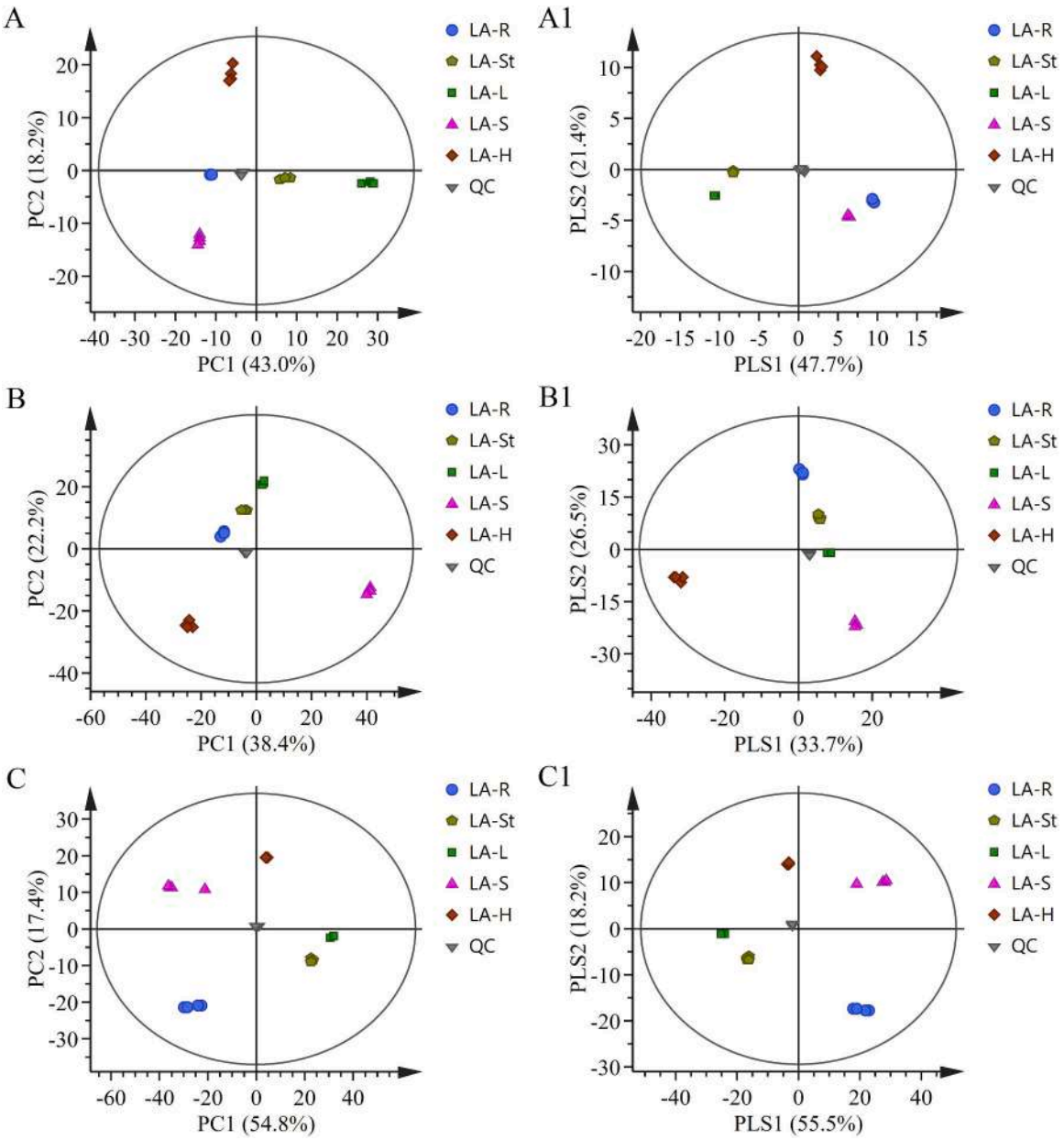

Fig. 1. PCA (A-C) and PLS-DA (A1-C1) analyses of VOs from GC–MS (A, A1) and NVEs from UPLC-QE-Orbitrap-HRMS in positive (B, B1) and negative (C, C1) ion modes. LA: *L. apetalum*, R: roots, St: stems, L: leaves, S: seeds, H: husks, QC: quality control.

information on the cytotoxicity of *L. apetalum* extracts remains lacking. In the present study, both VOs and NVEs at 100 μg/mL demonstrated varying degrees of cytotoxicity against different cancer cell lines (Fig. 3). Among the VO samples, the LA-H VO showed the strongest inhibition of HL-60 cell proliferation with inhibition rate of 47.41 %. LA-S VO displayed the highest activity against A549, HepG2, and MDA-MB-231 cells with inhibition ranging from 20.18 to 27.42 %. A previous study reported that seed oils of *L. sativum* at 100 μg/mL inhibited HepG2 cells by approximately 20 % (Al-Sheddi et al., 2013), which is comparable to the 20.18 % inhibition observed in the present study for the VO of *L. apetalum* seeds.

Among the NVE samples, LA-L NVE showed the highest inhibitory effects against HL-60 (57.45 %) and A549 (33.73 %) cells, partially supporting the nutraceutical value of *L. apetalum* leaf consumption. The IC_{50} vales of this sample was further determined to be 82.10 ± 4.79 μg/mL. In contrast, LA-H NVE exhibited the greatest activity against HepG2, MDA-MB-231, and SW480 cells, with inhibition rates ranging from 20.55 % to 32.03 %. The positive control DOX at 1.0 μg/mL displayed significant cytotoxicity with inhibition rates ranging from 50.19 to 92.00 %, confirming the effectiveness of the bioactivity assay system (**Table S3**). Previous studies have shown that alcoholic extracts of *L. sativum* seeds have also demonstrated cytotoxic activity against cancer cells such as HepG2 (Al-Sheddi et al., 2013). However, the impact of extraction solvents on the cytotoxic potential of *L. apetalum* extracts remains unexplored, highlighting an important direction for future research.

3.6. Antioxidant potential

The antioxidant potential of several *Lepidium* species, such as *L. sativum*, has been highlighted (Getahun et al., 2020), underscoring the importance of investigating antioxidant activity in less-explored species such as *L. apetalum*. In the present study, the antioxidant potential of *L. apetalum* was comprehensively evaluated across different plant parts

Table 2
Differential compounds identified by GC–MS for discriminating VOs from different parts of *L. apetalum*.

No.[a]	Compound	RI[b]	Class	VIP value[c]	*p* value[d]
102	*n*-Hexadecanoic acid	1977	Fatty acids	9.43	<0.001
40	Erucin	1440	Sulfur-containing compounds	9.13	<0.001
66	Phenylacetonitrile	1149	Nitrogen-containing compounds	8.76	<0.001
45	Dibenzyl disulfide	2082	Sulfur-containing compounds	6.66	<0.001
30	Benzenemethanethiol	1086	Sulfur-containing compounds	4.86	<0.001
27	Phytol	2111	Terpenoids	4.75	<0.001
39	Benzyl methyl disulfide	1395	Sulfur-containing compounds	4.10	<0.001
22	6,10,14-Trimethylpentadecan-2-one	1843	Terpenoids	3.92	<0.001
14	*trans*-*β*-Ionone	1464	Terpenoids	3.53	<0.001
11	Dehydrodihydroionone	1415	Terpenoids	3.37	<0.001
9	10-(Acetylmethyl)-(+)-3-carene	1391	Terpenoids	3.36	<0.001
34	5-(Methylsulfanyl) pentanenitrile	1206	Sulfur-containing compounds	3.32	<0.001
38	Benzyl isothiocyanate	1374	Sulfur-containing compounds	3.03	<0.001
55	Methyl hexadecanoate	1925	Esters	2.40	<0.001
70	1-Benzylpyrrole	1360	Nitrogen-containing compounds	1.90	<0.001
71	3-Nitrotoluene	1654	Nitrogen-containing compounds	1.89	<0.001
8	*α*-Longipinene	1334	Terpenoids	1.79	<0.001
68	1-Furfurylpyrrole	1185	Nitrogen-containing compounds	1.77	<0.001
47	Benzyl trisulfide	2354	Sulfur-containing compounds	1.61	<0.001
57	Methyl linolenate	2099	Esters	1.54	<0.001
23	Farnesyl acetone	1912	Terpenoids	1.47	<0.001
25	Isophytol	1947	Terpenoids	1.39	<0.001
36	6-(Methylthio) hexanenitrile	1320	Sulfur-containing compounds	1.35	<0.001
52	Methyl 7,10,13-hexadecatrienoate	1896	Esters	1.34	<0.001
42	3-Ethyl-2,4,5-trithiaoctane	1914	Sulfur-containing compounds	1.30	<0.001
44	Berteroin	1551	Sulfur-containing compounds	1.30	<0.001

[a] Compound numbers are consistent with those in Table 1, and compounds are ordered according to their VIP values.
[b] LRI: Linear retention index determined in this study using a C_7-C_{40} *n*-alkane standard.
[c] VIP: Variable importance in projection values obtained from PLS-DA analysis.
[d] *p*-values were calculated using ANOVA in IBM SPSS Statistics.

using DPPH and ABTS assays. For VOs, at a test concentration of 1600 μg/mL, LA-S and LA-H VOs exhibited stronger scavenging activity against both DPPH and ABTS radicals compared with the other samples, with inhibition rates ranging from 73.43 % to 96.47 % (Fig. 4A). The IC_{50} values for these two samples ranged from 143.69 to 874.43 μg/mL (Fig. 4B). A previous study reported that seed VOs of *L. apetalum* obtained by supercritical carbon dioxide extraction exhibited much weaker antioxidant activity, with IC_{50} values of 1000 μg/mL and 3750 μg/mL for DPPH and ABTS scavenging, respectively (Xu et al., 2011), suggesting that extraction methods significantly affect the bioactivity of volatile oils.

Compared with VOs, NVEs generally exhibited stronger antioxidant activity in both DPPH and ABTS assays, with inhibition rates ranging from 58.34 % to 92.04 % at 800 μg/mL (Fig. 4C). IC_{50} analysis indicated that LA-L, LA-S, and LA-H NVEs exhibited higher antioxidant activity, with low IC_{50} values (137.36–240.18 μg/mL for ABTS and 255.08–307.53 μg/mL for DPPH) (Fig. 4D). The antioxidant activities of NVEs, such as methanolic and ethanolic extracts, have previously been reported in several *Lepidium* species, including *L. sativum* (Chatoui et al., 2020). However, the present work is the first to demonstrate the antioxidant effects of NVEs from *L. apetalum*. Taken together, our findings highlight *L. apetalum* as a valuable source of natural antioxidants, particularly its seeds and husks.

3.7. Correlations between chemical compositions and biological activities

To further elucidate the associations between annotated metabolites and the observed bioactivities of *L. apetalum*, Pearson's correlation analysis was conducted, considering variations among different plant parts (Lin & Long, 2023). Differential compounds identified by GC–MS and LC-MS (Tables 2 and 3) were used to generate heatmaps (Fig. 5). For the GC–MS dataset, both positive and negative correlations between *L. apetalum* metabolites and bioactivities were observed (Fig. 5A). Several metabolites, including benzyl isothiocyanate (38), erucin (40), 3-ethyl-2,4,5-trithiaoctane (42), and 1-benzylpyrrole (70), showed positive correlations with anti-inflammatory activity. In contrast, VOs like *α*-longipinene (8) and dehydrodihydroionone (11) exhibited negative associations. Benzyl isothiocyanate and erucin are known for their anti-inflammatory effects in murine macrophages and mouse skin (Cho et al., 2013; Lee et al., 2009). The higher contents of erucin (44.19 %) and benzyl isothiocyanate (4.94 %) in LA-H (Table 1) may partly explain the stronger NO inhibition observed in this sample. Both compounds have also been reported to exert cytotoxic effects against HL-60 cells (Doudican et al., 2010; Jakubikova et al., 2005), supporting the positive correlation network revealed in the current study. However, the anti-inflammatory and anticancer properties of 3-ethyl-2,4,5-trithiaoctane and 1-benzylpyrrole remain unreported, underscoring the need for further investigation. Additionally, metabolites such as benzenemethanethiol (30), benzyl methyl disulfide (39), benzyl trisulfide (47), 1-furfurylpyrrole (68), and 3-nitrotoluene (71) displayed strong positive correlations with cytotoxicity against A549, HepG2, and MDA-MB-231 cells. They were also correlated with antioxidant activity in DPPH and ABTS assays. However, their anticancer and antioxidant activities have not been previously reported, highlighting promising directions for future research.

For LC-MS metabolites detected in the negative ion mode, several compounds showed strong positive correlations with NO inhibition (Fig. 5B). These included stearidonic acid (252) and embelin (543), both of which have well-documented anti-inflammatory activities (Basha et al., 2022; Sung et al., 2017). Other compounds, such as astilbin (283), hexamethylgossypetin (291), and flavanomarein (56), were strongly correlated with cytotoxic effects against A549, HepG2, and MDA-MB-231 cells, as well as with antioxidant activity (Fig. 5B). Although rosmarinic acid (482) has been recognized for cytotoxic, anti-inflammatory, and antioxidant activities (Nadeem et al., 2019), its correlations with the bioactivities of *L. apetalum* NVEs were weak or even negative. This discrepancy might due to the antagonistic effects from other constituents in the complex mixtures. In NVEs detected in the positive ion mode, both positive and negative associations were also observed (Fig. 5C). For example, indole-3-carboxaldehyde (42) and Phe-Pro (100) correlated closely with anti-inflammatory and antioxidant

Table 3
Differential compounds identified by LC-MS for discriminating NVEs from different parts of L. *apetalum*.

No.[a]	Compound	RT[b]	Class	VIP value[c]	*p* value[d]
Positive mode					
338	LPC(18:4)	405.0	Glycerophospholipids	1.78	<0.001
46	4-(4′-Methyl-[2,2′-bipyridin]-4-yl)butanoic acid	349.3	Alkanoids	1.77	<0.001
461	4-*O*-Feruloyl-D-quinic acid	260.0	Phenylpropanoids	1.73	<0.001
471	Hirsutenone	276.8	Phenylpropanoids	1.73	<0.001
374	PC(38:6)	606.9	Glycerophospholipids	1.71	<0.001
38	L-Oxonoreleagnine	288.0	Alkanoids	1.68	<0.001
118	Alanine	363.0	Amino acids and peptides	1.61	<0.001
353	LPC(18:1)	507.8	Glycerophospholipids	1.58	<0.001
503	Dihydrocurcumin	365.2	Phenylpropanoids	1.55	<0.001
317	Linarin	329.2	Flavonoids	1.54	<0.001
35	8-Hydroxycarbostyril	274.6	Alkanoids	1.52	<0.001
460	Ferulamide	259.3	Phenylpropanoids	1.51	<0.001
514	Idramantone	258.8	Terpenoids	1.50	<0.001
458	Prim-*O*-glucosylcimifugin	252.8	Phenylpropanoids	1.49	<0.001
176	3-Butynoic acid	76.8	Fatty acids and derivatives	1.48	<0.001
283	Cacticin	174.4	Flavonoids	1.44	<0.001
382	PC(38:2)	653.9	Glycerophospholipids	1.43	<0.001
28	Harmol	247.7	Alkanoids	1.43	<0.001
335	PC(18:1)	237.5	Glycerophospholipids	1.43	<0.001
3	4-Methylquinolin-2-ol	45.0	Alkanoids	1.42	<0.001
197	Pantothenol	198.5	Fatty acids and derivatives	1.41	<0.001
27	Aconine	243.6	Alkanoids	1.40	<0.001
100	Phe-Pro	250.1	Amino acids and peptides	1.39	<0.001
297	Kaempferol 3-*O*-*β*-sophoroside	290.0	Flavonoids	1.39	<0.001
73	*o*-Tyrosine	72.3	Amino acids and peptides	1.38	<0.001
42	Indole-3-carboxaldehyde	314.3	Alkanoids	1.38	<0.001
272	Stearamide	555.8	Fatty acids and derivatives	1.37	<0.001
294	Hexamethylgossypetin	285.1	Flavonoids	1.37	<0.001
487	6-Hydroxy-4-methyl-chromen-2-one	290.2	Phenylpropanoids	1.37	<0.001
289	4*H*-1-Benzopyran-4-one	266.0	Flavonoids	1.37	<0.001
243	Avocadyne 4-acetate	455.1	Fatty acids and derivatives	1.37	<0.001
391	1-Methylguanosine	162.2	Nucleosides	1.37	<0.001
516	Oleuropeinic acid	284.0	Terpenoids	1.37	<0.001
121	Threonine	377.4	Amino acids and peptides	1.37	<0.001
114	Proline	327.3	Amino acids and peptides	1.36	<0.001
51	Thiamine	371.4	Alkanoids	1.36	<0.001
45	Pipecolic acid	327.3	Alkanoids	1.36	<0.001
20	Mesaconine	215.7	Alkanoids	1.35	<0.001
296	Kaempferol 3-*O*-sophoroside	290.0	Flavonoids	1.35	<0.001
1	1-(1*H*-indol-3-yl)ethanone	33.8	Alkanoids	1.35	<0.001
293	6-Hydroxyluteolin 7-glucoside	278.6	Flavonoids	1.34	<0.001
29	Xanthurenic acid	254.2	Alkanoids	1.33	<0.001
332	PE(34:2)	173.8	Glycerophospholipids	1.33	<0.001
134	Stachyose	45.7	Carbohydrates	1.33	<0.001
392	2'-*O*-Methylguanosine	162.2	Nucleosides	1.32	<0.001
340	PC(8:0/8:0)	459.6	Glycerophospholipids	1.32	<0.001
125	Serine	394.0	Amino acids and peptides	1.32	<0.001
41	Stachydrine	311.3	Alkanoids	1.31	<0.001
445	Matairesinol	37.4	Phenylpropanoids	1.31	<0.001
160	*γ*-Linolenic acid	35.9	Fatty acids and derivatives	1.31	<0.001
564	Panglimycin C	310.4	Others	1.30	<0.001
303	Kaempferol 3-rungioside	306.5	Flavonoids	1.30	<0.001
81	Phenylalanine	102.2	Amino acids and peptides	1.30	<0.001
Negative mode					
134	Stachyose	45.7	Carbohydrates	1.83	<0.001
106	Tryptophan	282.3	Amino acids and peptides	1.81	<0.001
546	Ursolic acid	531.8	Terpenoids	1.68	<0.001
547	Caryophyllin	531.8	Terpenoids	1.68	<0.001
548	3-Epiursolic Acid	531.8	Terpenoids	1.68	<0.001
549	3-Epioleanolic acid	531.8	Terpenoids	1.68	<0.001
517	Isotoosendanin	302.0	Terpenoids	1.64	<0.001
278	*trans*-11-Eicosenoic acid	575.5	Fatty acids and derivatives	1.64	<0.001
279	Paullinic acid	575.5	Fatty acids and derivatives	1.64	<0.001
252	Arachidonic acid	485.0	Fatty acids and derivatives	1.55	<0.001
543	Nerylgeraniol-18-oic acid	486.3	Terpenoids	1.50	<0.001
291	Quercetin 3-gentiobioside	278.2	Flavonoids	1.50	<0.001
292	Baimaside	278.2	Flavonoids	1.50	<0.001
481	Isoacteoside	285.3	Phenylpropanoids	1.45	<0.001
482	Verbascoside	285.3	Phenylpropanoids	1.45	<0.001
483	Forsythiaside	285.3	Phenylpropanoids	1.45	<0.001
484	Acteoside	285.3	Phenylpropanoids	1.45	<0.001
355	LPE(18:1(9Z)/0:0)	512.2	Glycerophospholipids	1.39	<0.001
354	LPE(16:0)	508.9	Glycerophospholipids	1.39	<0.001

(*continued on next page*)

Table 3 (*continued*)

No.[a]	Compound	RT[b]	Class	VIP value[c]	*p* value[d]
530	Euscaphic acid	445.7	Terpenoids	1.38	<0.001
531	Caulophyllogenin	445.7	Terpenoids	1.38	<0.001
532	Asiatic acid	445.7	Terpenoids	1.38	<0.001
533	Arjunolic acid	445.7	Terpenoids	1.38	<0.001
534	Arjunic acid	445.7	Terpenoids	1.38	<0.001
535	Bayogenin	445.7	Terpenoids	1.38	<0.001
536	Ilexolic acid	445.7	Terpenoids	1.38	<0.001
283	Cacticin	174.4	Flavonoids	1.37	0.002
164	5*Z*,8*Z*,11*Z*-Eicosatrienoic acid	46.4	Fatty acids and derivatives	1.37	<0.001
270	*cis*-8,11,14-Eicosatrienoic acid	545.7	Fatty acids and derivatives	1.37	<0.001
55	Diglycine	41.9	Amino acids and peptides	1.37	<0.001
56	3-Ureidopropionic acid	41.9	Amino acids and peptides	1.37	<0.001
126	Asparagine	395.4	Amino acids and peptides	1.37	<0.001
385	Adenosine monophosphate	82.8	Nucleosides	1.33	<0.001
273	Oleic acid	556.9	Fatty acids and derivatives	1.30	<0.001
274	*trans*-Vaccenic acid	556.9	Fatty acids and derivatives	1.30	<0.001

[a] Compound numbers are consistent with those in Table S1, and compounds are ordered by VIP value.
[b] RT: Retention time (s).
[c] VIP: Variable importance in projection values obtained from PLS-DA analysis.
[d] *p*-values were calculated using ANOVA in IBM SPSS Statistics.

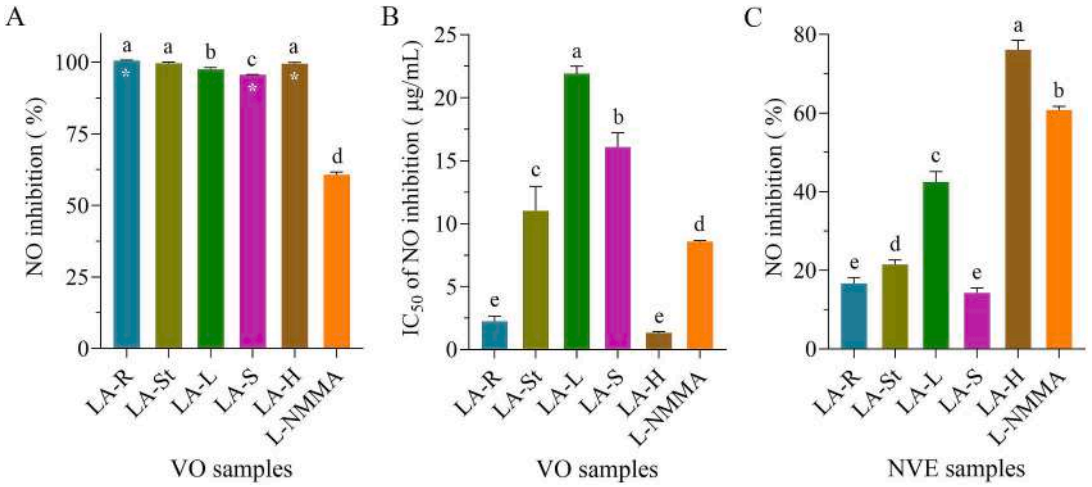

Fig. 2. Anti-inflammatory effects of VOs (A, B) and NVEs (C) from different parts of *L. apetalum*. Asterisks above columns indicate samples that were cytotoxic at the tested concentration. Different lowercase letters above the columns represent statistically significant differences among samples ($p < 0.05$). LA, *L. apetalum*; R, roots; St, stems; L, leaves; S, seeds; H, husks.

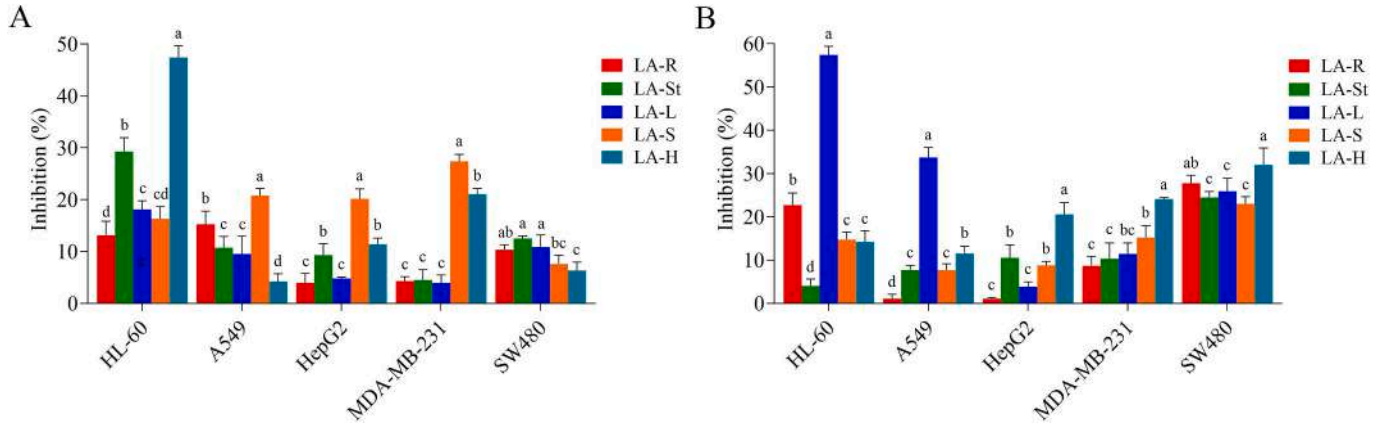

Fig. 3. Cytotoxic effects of VOs (A) and NVEs (B) from different plant parts of *L. apetalum* against five human cancer cell lines. Different lowercase letters above the bars indicate statistically significant differences ($p < 0.05$) among samples for the same cell line. LA: *L. apetalum*, R: roots, St: stems, L: leaves, S: seeds, H: husks.

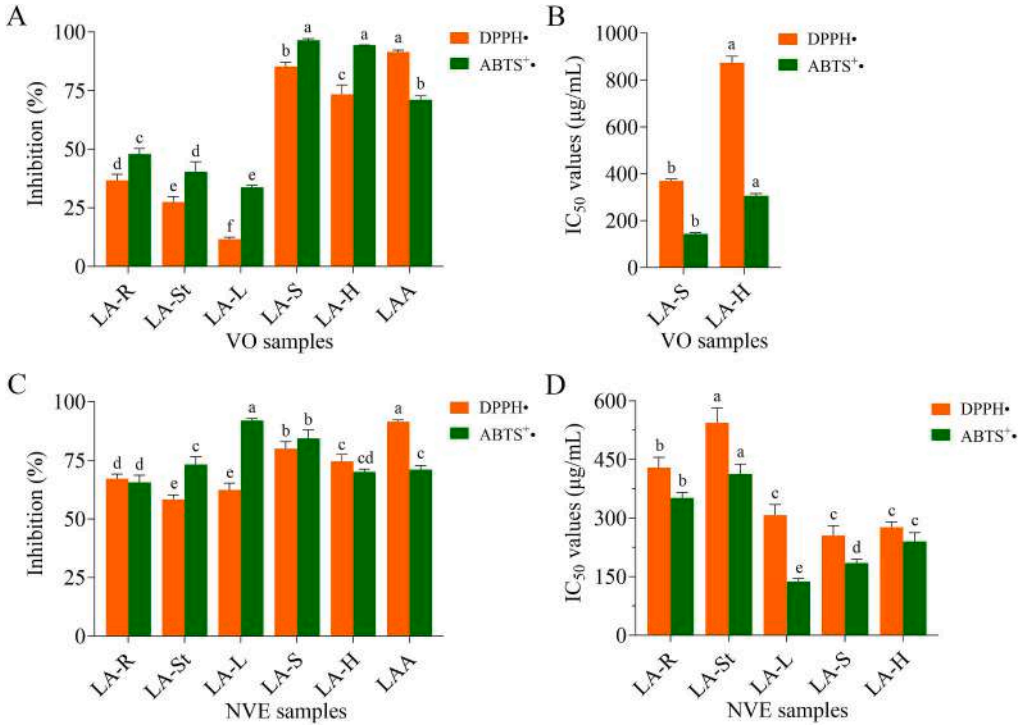

Fig. 4. Antioxidant potential of VOs (A, B) and NVEs (C, D) from different parts of *L. apetalum*. LA: *L. apetalum*, R: roots, St: stems, L: leaves, S: seeds, H: husks.

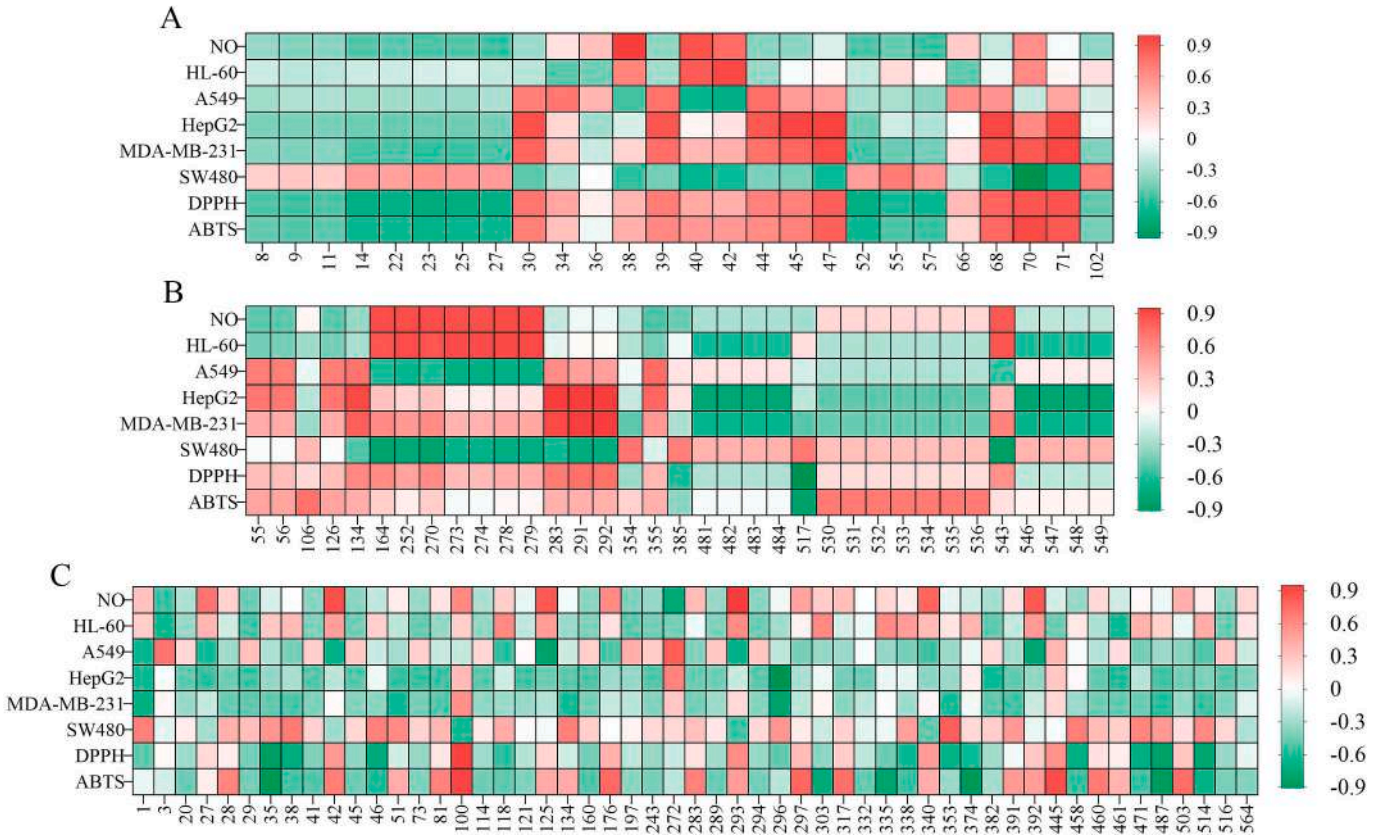

Fig. 5. Heatmaps showing correlations between bioactivities and differential metabolites detected by GC–MS (A) and UPLC-QE-Orbitrap-HRMS in negative (B) and positive (C) ion modes. Compound numbers in A correspond to Table 1, and those in B and C to Table S1. Values at the right indicate positive (above zero) or negative correlations (below zero) between metabolites and bioactivities.

effects, while L-oxonoreleagnine (38) and *cis*-11,14-eicosadienoic acid (272) were positively associated with cytotoxicity against cancer cell lines such as SW480 and A549. Conversely, metabolites like terphenyllin (564) exhibited only weak or negative correlations with bioactivities. Overall, these findings offer chemical insights into the bioactivities of *L. apetalum* and highlight potential pharmacologically active compounds, particularly those strongly correlated with observed bioactivities.

4. Conclusion

This study represents the first comprehensive analysis of the volatile oils and non-volatile extracts from different parts of *L. apetalum* using GC–MS and UPLC-QE-Orbitrap-HRMS-based metabolomics in combination with chemometrics and bioactivity evaluation. GC–MS identified 111 volatile compounds, while LC-MS annotated 583 metabolites using the in-house BiotreeDB database. The major volatiles included nitrogen- and sulfur-containing compounds, terpenoids, and fatty acids. In contrast, fatty acids and derivatives, amino acids and peptides, phenylpropanoids, glycerophospholipids, alkaloids, and flavonoids were commonly found in NVE samples. Chemometric analyses (PCA and PLS-DA) demonstrated significant metabolite variation among different plant parts. Several compounds, including fatty acids, flavonoids and terpenoids, were highlighted as key differential compounds responsible for the metabolite fluctuations. Bioactivity assays revealed marked differences between VOs and NVEs across plant parts, emphasizing the critical role of plant part selection for targeted therapeutic applications. Notably, root and husk VOs displayed the strongest anti-inflammatory potential with IC_{50} values lower than doxorubicin. Leaf NVE was the most cytotoxic against HL-60 cells, while both VOs and NVEs from seed and husk exhibited higher antioxidant activities in DPPH and ABTS assays. The observed bioactivity supported the consumption of *L. apetalum* from a nutraceutical perspective. Correlation analysis showed that differential metabolites were closely associated with bioactivities, identifying potential bioactive candidates for further investigation. Overall, this work provides a detailed phytochemical and pharmacological profile of *L. apetalum*, highlighting the potential of this species as a source of functional food ingredients. Additionally, the study demonstrates the potential of integrating metabolomics, chemometrics, and bioactivity evaluation to uncover bioactive compounds in food and medicinal plants.

CRediT authorship contribution statement

Fengke Lin: Writing – original draft, Methodology, Investigation, Funding acquisition, Formal analysis, Data curation, Conceptualization. **Qun Zhou:** Investigation, Data curation. **Guochen Lin:** Validation, Data curation. **Zihao Liu:** Investigation, Data curation. **Rui Zhao:** Investigation, Data curation. **Binsheng Luo:** Writing – review & editing, Validation, Supervision, Project administration, Funding acquisition, Formal analysis, Conceptualization.

Declaration of competing interest

The authors declare that they have no known competing financial interests or personal relationships that could have appeared to influence the work reported in this paper.

Acknowledgements

This study was supported by the National Natural Science Foundation of China (32300325 and 32400306), the Special Project of the Lushan Botanical Garden (No. 2024ZWZX06), and the “Xuncheng Talents” Program of Jiujiang City (No. JJXC2023136).

Appendix A. Supplementary data

Supplementary data to this article can be found online at https://doi.org/10.1016/j.fochx.2025.103376.

Data availability

Data will be made available on request.

References

Abraham, E. J., & Kellogg, J. (2021). Chemometric-guided approaches for profiling and authenticating botanical materials. *Frontiers in Nutrition, 8*, Article 780228. https://doi.org/10.3389/fnut.2021.780228

Adams, R. P. (2017). *Identification of essential oil components by gas chromatography/mass spectrometry (ed. 4.1)*. Allured Publishing.

Afsharypuor, S., & Hadi, M. (2006). Volatile constituents of the seeds, roots and non-flowering aerial parts of *Lepidium satvium* L. *Journal of Essential Oil Research, 18*, 495–496. https://doi.org/10.1080/10412905.2006.9699151

Alagawany, M., Abd El-Hack, M. E., Farag, M. R., Gopi, M., Karthik, K., Malik, Y. S., & Dhama, K. (2017). Rosmarinic acid: Modes of action, medicinal values and health benefits. *Animal Health Research Reviews, 18*, 167–176. https://doi.org/10.1017/S1466252317000081

Al-Sheddi, E. S., Farshori, N. N., Al-Oqail, M. M., Musarrat, J., Al-Khedhairy, A. A., & Siddiqui, M. A. (2013). Evaluation of cytotoxicity and oxidative stress induced by alcoholic extract and oil of *Lepidium sativum* seeds in human liver cell line HepG2. *African Journal of Biotechnology, 12*, 3854–3863.

Al-Shehbaz, I. A. (2012). A generic and tribal synopsis of the Brassicaceae (Cruciferae). *Taxon, 61*, 931–954. https://doi.org/10.1002/tax.615002

Al-Snafi, A. (2019). Chemical constituents and pharmacological effects of *Lepidium sativum*-a review. *International Journal of Current Pharmaceutical Research, 11*, 1–10. https://doi.org/10.22159/ijcpr.2019v11i6.36338

Basha, N. J., Basavarajaiah, S., Baskaran, S., & Kumar, P. (2022). A comprehensive insight on the biological potential of embelin and its derivatives. *Natural Product Research, 36*, 3054–3068. https://doi.org/10.1080/14786419.2021.1955361

Carvalho, F. V., Santana, L. F., da Silva, V. D. A., Costa, S. L., Zambotti-Villelae, L., Colepicolo, P., Ferraz, C. G., & Ribeiro, P. R. (2021). Combination of a multiplatform metabolite profiling approach and chemometrics as a powerful strategy to identify bioactive metabolites in *Lepidium meyenii* (*Peruvian maca*). *Food Chemistry, 364*, Article 130453. https://doi.org/10.1016/j.foodchem.2021.130453

Chatoui, K., Harhar, H., El Kamli, T., & Tabyaoui, M. (2020). Chemical composition and antioxidant capacity of *Lepidium sativum* seeds from four regions of Morocco. *Evidence-based Complementary and Alternative Medicine, 2020*, Article 7302727. https://doi.org/10.1155/2020/7302727

Cho, H. J., Lee, K. W., & Park, J. H. Y. (2013). Erucin exerts anti-inflammatory properties in murine macrophages and mouse skin: Possible mediation through the inhibition of NFκB signaling. *International Journal of Molecular Sciences, 14*, 20564–20577. https://doi.org/10.3390/ijms141020564

Commission of Chinese Ethnomedicines. (2005). *Lepidium apetalum* Willd. In M. Jia, & X. Li (Eds.), *Zhong Guo Min Zu Yao Zhi Yao (Chinese ethnomedicines)* (p. 367). China Medical Science Press.

Doudican, N. A., Bowling, B., & Orlow, S. J. (2010). Enhancement of arsenic trioxide cytotoxicity by dietary isothiocyanates in human leukemic cells via a reactive oxygen species-dependent mechanism. *Leukemia Research, 34*, 229–234. https://doi.org/10.1016/j.leukres.2009.05.017

Gallegos-Saucedo, R., Barrios-García, T., Valdez-Morales, E. E., Cabañas-García, E., Barajas-Espinosa, A., Gómez-Aguirre, Y. A., & Guerrero-Alba, R. (2024). Cytotoxic activity of *Lepidium virginicum* L. methanolic extract on human colorectal cancer cells, Caco-2, through p53-mediated apoptosis. *Molecules, 29*, 3920. https://doi.org/10.3390/molecules29163920

Gargi, B., Semwal, P., Jaiswal, D. K., Painuli, S., Trivedi, V. L., Tripathi, V., & Rai, N. (2025). Impact of circadian rhythm and seasonal variability on the essential oil of Allium stracheyi baker from Uttarakhand, Himalaya. *Food Chemistry: X, 29*, Article 102720. https://doi.org/10.1016/j.fochx.2025.102720

Getahun, T., Sharma, V., & Gupta, N. (2020). Chemical composition, antibacterial and antioxidant activities of oils obtained by different extraction methods from *Lepidium sativum* L. seeds. *Industrial Crops and Products, 156*, Article 112876. https://doi.org/10.1016/j.indcrop.2020.112876

Gong, J., Zheng, X., Hao, J., Zhang, Y., Li, C., Cao, Y., Kuang, H., & Wei, W. (2015). Analysis on essential oil in seeds of *Lepidium apetalum* Willd. by GC-MS. *World Science and Technology/Modernization of Traditional Chinese Medicine and Materia Medica, 17*, 499–506.

Gullón, B., Lú-Chau, T. A., Moreira, M. T., Lema, J. M., & Eibes, G. (2017). Rutin: A review on extraction, identification and purification methods, biological activities and approaches to enhance its bioavailability. *Trends in Food Science & Technology, 67*, 220–235. https://doi.org/10.1016/j.tifs.2017.07.008

Jakubikova, J., Bao, Y., & Sedlák, J. (2005). Isothiocyanates induce cell cycle arrest, apoptosis and mitochondrial potential depolarization in HL-60 and multidrug-resistant cell lines. *Anticancer Research, 25*, 3375–3386.

Kim, K.-Y., Kang, Y.-M., Lee, A., Kim, Y.-J., Kim, K.-H., & Hwang, Y.-H. (2024). Hydroethanolic extract of *Lepidium apetalum* Willdenow alleviates dextran sulfate sodium-induced colitis by enhancing intestinal barrier integrity and inhibiting

oxidative stress and inflammasome activation. *Antioxidants, 13*, 795. https://doi.org/10.3390/antiox13070795

Lahiri, B., & Rani, R. (2020). Garden cress seeds: Chemistry, medicinal properties, application in dairy and food industry: A review. *Emergent Life Sciences Research, 6*, 1–4. https://doi.org/10.31783/elsr.2020.620104

Lee, Y. M., Seon, M. R., Cho, H. J., Kim, J.-S., & Park, J. H. Y. (2009). Benzyl isothiocyanate exhibits anti-inflammatory effects in murine macrophages and in mouse skin. *Journal of Molecular Medicine, 87*, 1251–1261. https://doi.org/10.1007/s00109-009-0532-6

Li, S., Zhang, S., Li, X., Zhou, S., Ma, J., Zhao, X., Zhang, Q., & Yin, X. (2023). Determination of multi-mycotoxins in vegetable oil via liquid chromatography-high resolution mass spectrometry assisted by a complementary liquid–liquid extraction. *Food Chemistry: X, 20*, Article 100887. https://doi.org/10.1016/j.fochx.2023.100887

Lin, F., Kennelly, E. J., Linington, R. G., & Long, C. (2023). Comprehensive metabolite profiling of two edible Garcinia species based on UPLC-ESI-QTOF-MS^{E} coupled with bioactivity assays. *Journal of Agricultural and Food Chemistry, 71*, 7604–7617. https://doi.org/10.1021/acs.jafc.2c08372

Lin, F., & Long, C. (2023). GC-TOF-MS-based metabolomics correlated with bioactivity assays unveiled seasonal variations in leaf essential oils of two species in *Garcinia* L. *Industrial Crops and Products, 194*, Article 116356. https://doi.org/10.1016/j.indcrop.2023.116356

Lin, F., Recchia, M. J., Clark, T. N., Kennelly, E. J., Linington, R. G., & Long, C. (2025). Metabolite profiling and characterization of potential anticancer constituents from *Garcinia subfalcata* using UPLC-IMS-QTOF-MS. *Food Chemistry, 465*, Article 141900. https://doi.org/10.1016/j.foodchem.2024.141900

Mottaghipisheh, J., Taghrir, H., Boveiri Dehsheikh, A., Zomorodian, K., Irajie, C., Mahmoodi Sourestani, M., & Iraji, A. (2021). Linarin, a glycosylated flavonoid, with potential therapeutic attributes: A comprehensive review. *Pharmaceuticals, 14*, 1104. https://doi.org/10.3390/ph14111104

Nadeem, M., Imran, M., Aslam Gondal, T., Imran, A., Shahbaz, M., Muhammad Amir, R., … Hussain, G. (2019). Therapeutic potential of rosmarinic acid: A comprehensive review. *Applied Sciences, 9*, 3139. https://doi.org/10.3390/app9153139

Pang, S., Piao, X., Zhang, X., Chen, X., Zhang, H., Jin, Y., Li, Z., & Wang, Y. (2023). Discrimination for geographical origin of *Panax quinquefolius* L. using UPLC Q-Orbitrap MS-based metabolomics approach. *Food Science & Nutrition, 11*, 4843–4852. https://doi.org/10.1002/fsn3.3461

Ravi, L., & Krishnan, K. (2017). Research article cytotoxic potential of *n*-hexadecanoic acid extracted from *Kigelia pinnata* leaves. *Asian Journal of Cell Biology., 12*, 20–27. https://doi.org/10.3923/ajcb.2017.20.27

Ren, Y., Lin, F., Meng, J., Liu, Y., Li, Y., Zhao, W., Zhao, R., Zhu, D., & Liu, Y. (2025). Characterization of potential bioactive molecules in *Fissistigma polyanthum* using UPLC-ESI-QTOF-MS-based metabolomics integrated with chemometrics approaches. *Journal of Chromatography A, 1746*, Article 465804. https://doi.org/10.1016/j.chroma.2025.465804

Selek, S., Koyuncu, I., Caglar, H. G., Bektas, I., Yilmaz, M. A., Gonel, A., & Akyuz, E. (2018). The evaluation of antioxidant and anticancer effects of *Lepidium sativum* Subsp Spinescens L. methanol extract on cancer cells. *Cellular and Molecular Biology, 64*, 72–80. http://orcid.org/0000-0003-1235-3957.

Sharma, N., Tiwari, N., Vyas, M., Khurana, N., Muthuraman, A., & Utreja, P. (2020). An overview of therapeutic effects of vanillic acid. *Plant Arch, 20*, 3053–3059.

Shi, P., Chao, L., Wang, T., Liu, E., Han, L., Zong, Q., Li, X., Zhang, Y., & Wang, T. (2015). New bioactive flavonoid glycosides isolated from the seeds of *Lepidium apetalum* Willd. *Fitoterapia, 103*, 197–205. https://doi.org/10.1016/j.fitote.2015.04.007

Sung, J., Jeon, H., Kim, I.-H., Jeong, H. S., & Lee, J. (2017). Anti-inflammatory effects of stearidonic acid mediated by suppression of NF-κB and MAP-kinase pathways in macrophages. *Lipids, 52*, 781–787. https://doi.org/10.1007/s11745-017-4278-6

Tellez, M. R., Khan, I. A., Kobaisy, M., Schrader, K. K., Dayan, F. E., & Osbrink, W. (2002). Composition of the essential oil of *Lepidium meyenii* (Walp.). *Phytochemistry, 61*, 149–155. https://doi.org/10.1016/S0031-9422(02)00208-X

Wu, X., Li, M., Yang, S., Dong, J., Pan, W., Ning, Y., Hua, X., Dong, D., & Liang, D. (2023). Liver metabolic dysregulation induced by polypropylene nano-and microplastics in *Nile tilapia* using internal extractive electrospray ionization mass spectrometry. *Analytical Chemistry, 95*, 7863–7871. https://doi.org/10.1021/acs.analchem.2c05672

Xu, W., Chu, K., Li, H., Chen, L., Zhang, Y., & Tang, X. (2011). Extractionof *Lepidium apetalum* seed oil using supercritical carbon dioxide and anti-oxidant activity of the extracted oil. *Molecules, 16*, 10029–10045. https://doi.org/10.3390/molecules161210029

Yuan, P., Zheng, X., Li, M., Ke, Y., Fu, Y., Zhang, Q., Wang, X., & Feng, W. (2017). Two sulfur glycoside compounds isolated from *Lepidium apetalum* willd protect NRK52e cells against hypertonic-induced adhesion and inflammation by suppressing the MAPK signaling pathway and RAAS. *Molecules, 22*, 1956. https://doi.org/10.3390/molecules22111956

Zhang, B. (2000). The quiet rise of three kinds of leafy vegetables. *Beijing Agricultural Sciences, 18*, 34–35.

Zhang, K., Zhang, Y., Ji, Y., Walck, J. L., & Tao, J. (2020). Seed biology of *Lepidium apetalum* (Brassicaceae), with particular reference to dormancy and mucilage development. *Plants, 9*, 333. https://doi.org/10.3390/plants9030333

Zhao, H., Wang, X., & Lu, J. (2005). Study on the volatile and fixed oil components in seeds of *Lepidium apetalum*. *Chinese Traditional and Herbal Drugs, 36*, 827–828.